Letter

Quantitative determination of the confinement and deconfinement of spinons in the anomalous spectra of antiferromagnets via the entanglement entropy

Zhao-Yang Dong [1], Wei Wang,[2,*] Zhao-Long Gu,[3,†] and Jian-Xin Li[3,4,‡]

[1]*Department of Applied Physics, Nanjing University of Science and Technology, Nanjing 210094, China*

[2]*School of Science, Nanjing University of Posts and Telecommunications, Nanjing 210023, China*

[3]*National Laboratory of Solid State Microstructures and Department of Physics, Nanjing University, Nanjing 210093, China*

[4]*Collaborative Innovation Center of Advanced Microstructures, Nanjing University, Nanjing 210093, China*

(Received 5 July 2021; accepted 8 November 2021; published 17 November 2021)

We introduce an entanglement entropy analysis to quantitatively identify the confinement and deconfinement of the spinons in the spin excitations of quantum magnets. Our proposal is implemented by the parton construction of a honeycomb-lattice antiferromagnet exhibiting high-energy anomalous spectra. To obtain the quasiparticles of spin excitations for entanglement entropy calculations, we develop an effective Hamiltonian using the random phase approximation. We elaborate quantitatively the deconfinement-to-confinement transition of spinons in the anomalous spectra with the increase of the Hubbard interaction, indicating the avoided fractionalization of magnons in the strong interaction regime. Meanwhile, the Higgs mode at the Γ' point is fractionalized into four degenerate spinons, although it appears as a sharp well-defined peak in the spectra. Our work extends our understanding of the deconfinement of the spinon and its coexistence with the magnon in quantum magnets.

DOI: 10.1103/PhysRevB.104.L180406

The nature of the ground states and their respective elementary spin excitations resides at the center of the field of quantum magnetism. For quantum magnets with strong frustrations, quantum fluctuations can suppress the formation of local magnetic orders, thus, exotic spin liquid phases can be stabilized, with deconfined spinons as the elementary excitations [1]. On the other hand, for quantum magnets in the weak-frustration or frustration-free regime, the system hosts long-range magnetic orders, and the low-energy physics can be captured quite well by the semiclassical approach, i.e., the spin wave theory (SWT), where the elementary excitations are well-defined magnons. However, this does not imply that the quantum fluctuations are negligible for ordered quantum magnets. In fact, the semiclassical ordered states are not their exact ground states in the presence of fluctuations which usually reduce the magnitude of the local magnetic order significantly [2,3]. The ground state of an ordered quantum magnet may be close to a spin liquid state, such as the resonating-valence-bond (RVB) state [4].

Recent studies on the spin excitation spectra further reveal the quantum nature of the magnetically ordered quantum magnets. Compared to the SWT predictions, inelastic neutron scattering experiments on the square-lattice antiferromagnetic (AF) compounds [5–7] uncovered a remarkable anomaly at $(\pi, 0)$ of the Brillouin zone (BZ) in the high-energy spectra, where the energies of the transverse spin excitations are renormalized downward to form a rotonlike minimum. Meanwhile, the sharp well-defined magnonic modes disappear around this point with a dim broad continuum left. Similar anomalous behaviors were also observed in other AF compounds on different two-dimensional lattices experimentally [8–17]. Such anomalies indicate that additional spin fluctuations, such as those in the adjacent spin liquid phase, would survive in the AF ordered ground state. To appropriately capture the physics of the spin excitations at all energies, it appears more suitable to describe the ordered quantum magnets in terms of spinons [18–20]. In this scenario, the magnon is a bound state of two spinons lying in the gap of the two-spinon continuum. In fact, based on the variational RVB ansatz with magnetic orders, the anomaly in the high energy spin excitation spectra is attributed to the deconfinement of spin-1/2 spinons [6,21–25]. This scenario is supported by various numerical studies [6,19,21–32], including the unbiased large-scale quantum Monte Carlo simulations [31].

In this spinon-based interpretation, the main evidence in favor of the deconfinement of spinons in the anomalous spectra of ordered magnets is that the continuum can be continuously evolved into that appearing in a neighboring disordered state by varying some model parameters, which indeed consists of deconfined particle-hole spinon pairs [21,23,31]. However, with a fixed given set of parameters, the deconfinement can only be phenomenologically determined by the evolution of the spectral line shape from a sharp Lorentzian peak to a broad continuum [21–23,31]. In nature, it still remains elusive to distinguish spinons from magnons when they are coupled in the anomalous spin spectra. In this Letter we propose the entanglement entropy (EE) of a spin excitation as the hallmark to identify the deconfinement of spinons in the excitation spectra of quantum magnets unambiguously and quantitatively.

*wwang@njupt.edu.cn

†waltergu1989@gmail.com

‡jxli@nju.edu.cn

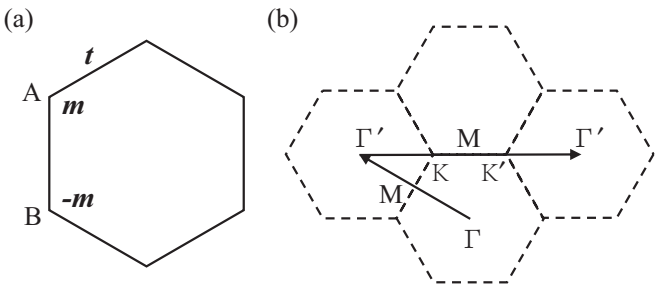

FIG. 1. (a) Illustration of Eq. (1) in the honeycomb lattice. A and B denote the two sublattices of the honeycomb lattice. t is RVB hopping parameter and m denotes the order parameter of the AF order. (b) High symmetry points in the Brillouin zone.

The physics underlaying our proposal is as following. For a system with N spins, a state is always written as $|\psi\rangle = \sum_{\{n\}} a(\{n\})|\{n\}\rangle_\uparrow \otimes |\{N\}-\{n\}\rangle_\downarrow$, where $|\{n\}\rangle_\sigma$ indicate the configuration of a state with n spin σ. Since it is the Schmidt decomposition with respect to the separation in the spin space, the EE of the state is $\sum_{\{n\}} -a(\{n\})^2 \ln[a(\{n\})^2]$ and its difference from the ground state can be defined to analysis the nature of spin excitations [43]. In the spinon scenario, spin excitations can be represented by quasiparticles $\widehat{\Psi} = \sum_{\{\alpha\}\{\beta\}} \psi(\{\alpha\},\{\beta\}) \prod_{i\in\{\alpha\}} d_i^\dagger \otimes \prod_{j\in\{\beta\}} d_j$, where $i(j)$ includes all the indexes of the spinon represented by the operator $d_{i(j)}$. A more convenient EE of quasiparticles can be obtained from a singular value decomposition with respect to the separation of particle and hole spinons. As one of the intrinsic attributes, the scalings of EEs could characterize the spin excitations. The EEs of magnons, for which the particle-hole pairs are confined to form bound states, are logarithmically divergent in the thermodynamic limit, while the EEs of the modes in the spinon continuum, which can be decomposed into relatively free particle and hole spinons, converge to constants. Thus, one only needs the wave functions or quasiparticles of states to perform such EE analysis. To illustrate the application of our proposal, here we carry out the random phase approximation (RPA) calculations of the honeycomb-lattice antiferromagnet in the weak-frustration regime exhibiting high-energy anomalous spectra, which is relevant to the recent experiments on $YbCl_3$ and $YbBr_3$ [14,15,17]. We elaborate quantitatively the deconfinement-to-confinement transition of spinons in the anomalous spectra with the increase of the Hubbard interaction, indicating the avoided fractionalization of magnons in the strong interaction regime. We find strikingly that the Higgs mode at the Γ' point is always fractionalized. Our work reveals the insufficiency of the spectral perspective and provides an quantitatively accurate judgment on the deconfinement of spinons.

We start with the J_1-J_2 Heisenberg model of the honeycomb lattice. Several structures could be close to the AF phase [33–35] with the introduction of frustrations, and it has been shown by the mean-field theory that the most energetically favorite one is the SU(2) RVB ansatz [36]. Therefore, we adopt this ansatz with the AF order [see Fig. 1(a)], and the mean-field Hamiltonian for the J_1-J_2 model is then given by

$$H_{\mathrm{MF}} = t \sum_{\langle ij\rangle\sigma} f_{i\sigma}^\dagger f_{j\sigma} + \sum_{i\sigma\sigma'} m_i f_{i\sigma}^\dagger \sigma^z_{\sigma\sigma'} f_{i\sigma'}. \tag{1}$$

where $f_{i\sigma}$ is the fermionic spinon operator satisfying $\mathbf{S_i} = 1/2 \sum_{\sigma\sigma'} f_{i\sigma}^\dagger \boldsymbol{\sigma}_{\sigma\sigma'} f_{i\sigma'}$ at site i, in which σ is the spin index and $\boldsymbol{\sigma}$ is the Pauli matrix. Here $t = -0.158J_1$ is the SU(2) RVB hopping parameter and $m_A = -m_B = m = 0.191J_1$ is the self-consistent mean-field solution of the AF order parameter with $J_2 = 0.3J_1$ [36]. The SU(2) RVB ansatz implies the fluctuations of the plaquette valence bonds [37–41]. We will focus on the spin-liquid-like fluctuations surviving in the AF phase, the spiral spin orders [40,42] are not included. Then, Eq. (1) can be diagonalized with $f_{\mathbf{k}\alpha\sigma} = \sum_{\gamma\sigma'} u_{\alpha\gamma}^{\sigma\sigma'}(\mathbf{k}) d_{\mathbf{k}\gamma\sigma'}$. $u_{\alpha\gamma}^{\sigma\sigma'}(\mathbf{k})$ are the matrix elements of $U(\mathbf{k})$ [36], where α denotes the sublattice index and γ denotes the band index. And the spinon dispersion is obtained $\varepsilon(\mathbf{k}) = \sqrt{|t\lambda(\mathbf{k})|^2 + m^2}$, where $\lambda(\mathbf{k}) = (1 + e^{i\mathbf{k}\cdot r_1} + e^{i\mathbf{k}\cdot r_2})$ [36].

Going beyond the mean-field level, RPA can be applied [22,28]. To represent the fluctuations in the spin density channel, we introduce the Heisenberg interaction $J_{\mathrm{eff}}\mathbf{S_i}\cdot\mathbf{S_j}$ between the spinons on the nearest-neighbor sites. We also take into account the Hubbard interaction $U_{\mathrm{eff}} n_{i\uparrow} n_{i\downarrow}$ to simulate partially the effect of the no-double-occupancy constraint on spinons. They satisfy $J_{\mathrm{eff}} + 2U_{\mathrm{eff}}/3 = 0.4J_1$ in the self-consistent calculation. In the following, we take the proportion of the Hubbard interaction denoted by a as the variable to show the results, i.e., we take $U_{\mathrm{eff}} = a0.6J_1$, $J_{\mathrm{eff}} = (1-a)0.4J_1$. It is noted that both U_{eff} and J_{eff} should be understood as phenomenological parameters here, which are introduced to mimic the gauge fluctuation and induce a static magnetic order in the system simultaneously [22].

With these interactions, the spin susceptibility $\boldsymbol{\chi}$ is obtained in the RPA approach,

$$\boldsymbol{\chi}(\mathbf{q},\omega) = \frac{\boldsymbol{\chi}^{\mathbf{0}}(\mathbf{q},\omega)}{\mathbf{I} + \mathbf{V}(\mathbf{q})\boldsymbol{\chi}^{\mathbf{0}}(\mathbf{q},\omega)}, \tag{2}$$

where the bare susceptibility $\boldsymbol{\chi}^{\mathbf{0}}$ is the standard Lindhard function for the noninteracting fermionic system described by Eq. (1) (see Eq. (S3) in [36]). $\mathbf{V}(\mathbf{q}) = -U_{\mathrm{eff}}\mathbf{I} + \mathbf{J}(\mathbf{q})$, $\mathbf{J}(\mathbf{q})$ is given by

$$\mathbf{J}(\mathbf{q}) = \begin{pmatrix} 0 & J_{\mathrm{eff}}\mathbf{I_{3\times 3}}\lambda(\mathbf{q}) \\ J_{\mathrm{eff}}\mathbf{I_{3\times 3}}\lambda^*(\mathbf{q}) & 0 \end{pmatrix}.$$

The spectral functions of the transverse/longitudinal spin excitations are related to $\boldsymbol{\chi}$ via $I^{-+/zz}(\mathbf{q},\omega) = \mathrm{Im}[\chi^{-+/zz}(\mathbf{q},\omega + i0^+)]/\pi$.

In the zero-temperature RPA, the spinon particle-hole operators can be approximately regarded as quasibosonic operators $b^\dagger_{\mathbf{kq}\sigma\sigma'} \simeq d^\dagger_{\mathbf{k}-\mathbf{q}1\sigma} d_{\mathbf{k}2\sigma'}$. Thus, we can develop an effective Hamiltonian about the spin excitations from RPA [36],

$$\begin{aligned} H_{\mathrm{eff}}(\mathbf{q}) = \sum_{\mathbf{k}\sigma\sigma'} &\{[\varepsilon(\mathbf{k}-\mathbf{q}) + \varepsilon(\mathbf{k})] b^\dagger_{\mathbf{kq}\sigma\sigma'} b_{\mathbf{kq}\sigma\sigma'} \\ &+ [\varepsilon(\mathbf{k}+\mathbf{q}) + \varepsilon(\mathbf{k})] b_{\mathbf{k}\bar{\mathbf{q}}\sigma\sigma'} b^\dagger_{\mathbf{k}\bar{\mathbf{q}}\sigma\sigma'}\} \\ &+ \Phi^\dagger_{\mathbf{q}} \bar{U}^\dagger_{\mathbf{q}} V_{\mathbf{q}} \bar{U}_{\mathbf{q}} \Phi_{\mathbf{q}}, \end{aligned}$$

where $\Phi^\dagger_{\mathbf{q}} = (\cdots b^\dagger_{\mathbf{kq}\sigma\sigma'} \cdots b_{\mathbf{k}\bar{\mathbf{q}}\sigma\sigma'} \cdots)$, $\bar{U}_{\mathbf{q}} = \mathbf{I}_{N_{\mathbf{k}}\times N_{\mathbf{k}}} \otimes U^*(\mathbf{k}) \otimes U(\mathbf{k}-\mathbf{q})$, and $V_{\mathbf{q}}$ is the coefficient matrix of the Fourier transform of the Hubbard and Heisenberg terms $[V_{\mathbf{q}}]_{\mathbf{k}\alpha\beta;\mathbf{k}'\alpha'\beta'} f^\dagger_{\mathbf{k}-\mathbf{q}\alpha} f_{\mathbf{k}\beta} f^\dagger_{\mathbf{k}'\alpha'} f_{\mathbf{k}'-\mathbf{q}\beta'}$. Then the ith quasiparticle $\widehat{\Psi}_i(\mathbf{q})$ of the spin excitations is solved from H_{eff} as a linear

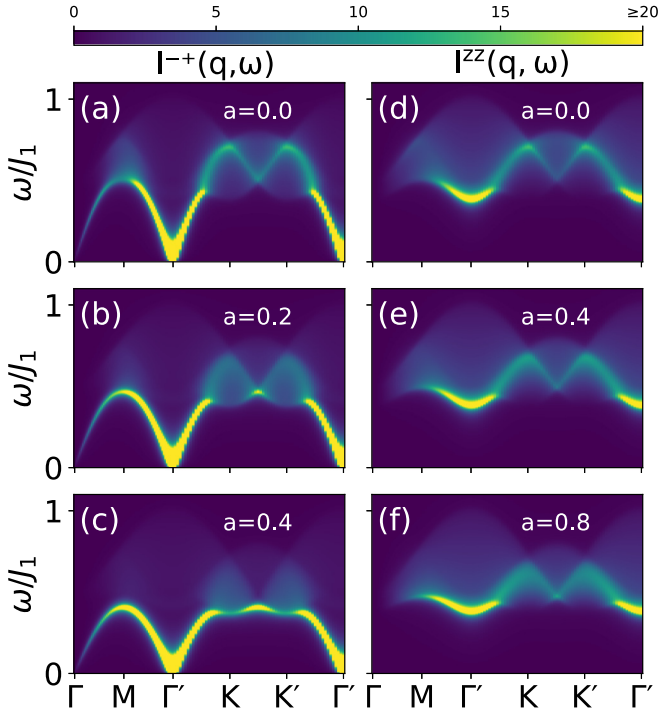

FIG. 2. Spectral functions of the (a)–(c) transverse and (d)–(f) longitudinal spin excitations along the Γ-M-Γ′-K-K′-Γ′ path denoted in Fig. 1(b).

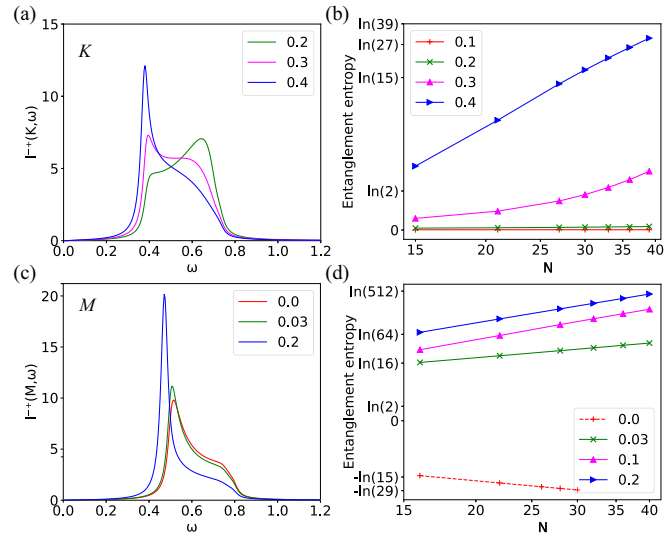

FIG. 3. On the left: transverse spectral functions at (a) K and (c) M. On the right: scalings with system size N of the EEs of the lowest transverse modes at (b) K and (d) M. The legends in the figures indicate the increasing of a by different colors. The dashed lines denote the EEs of degenerate modes.

combination of the products of such particle-hole spinon pairs:

$$\widehat{\Psi}_i(\mathbf{q}) = \sum_{\mathbf{k}\gamma\sigma\sigma'} \psi_{i\mathbf{k}\gamma\sigma\sigma'}(\mathbf{q}) d^{\dagger}_{\mathbf{k}-\mathbf{q}\gamma\sigma} \otimes d_{\mathbf{k}\bar{\gamma}\sigma'}. \tag{3}$$

Since the independence of the transverse and longitudinal spin dynamics, the spin indexes σ and σ' are binding for each excitations. Thus, Eq. (3) would be reduced to the Schmidt decomposition of particle and hole spinons. Though the coefficient $\psi_{i\mathbf{k}\sigma\sigma'}(\mathbf{q})$ is not normalized, it can be viewed as a vector, whose α norm is well defined, thus, the Rényi entropy reads

$$S_i(\mathbf{q}) = \frac{1}{1-\alpha} \ln\Big(\sum_{\mathbf{k}\gamma\sigma\sigma'} |\psi_{i\mathbf{k}\gamma\sigma\sigma'}(\mathbf{q})|^{2\alpha}\Big). \tag{4}$$

Now let us turn to the numerical results of spectra. In Figs. 2(a)–2(c) the transverse spectra of the AF phase with SU(2) RVB fluctuations along the Γ-M-Γ′-K-M-K′-Γ′ path in the BZ [see Fig. 1(b)] are presented with three typical a values. The spectra are composed of a dim broad spinon particle-hole continuum and a bright branch of magnons. The energies of the spinon pairs are $\omega_{\mathbf{k}}(\mathbf{q}) = \varepsilon(\mathbf{k}-\mathbf{q}) + \varepsilon(\mathbf{k})$, thus the continuum is gapped with the bottom lying at Γ/K. The magnons appear below the spinon continuum with a linear dispersion relation away from the gapless Goldstone mode at Γ/Γ' as well as a divergent intensity at Γ′, which is in agreement with the SWT. However, the high-energy magnonic spectra exhibit distinct behaviors along the BZ boundary from K to M, compared to the SWT predictions. When the Hubbard interaction is absent [Fig. 2(a)], the bright magnons are scattered into the continuum as the dispersion ascends to K, and are completely absent along the K-M line. As the Hubbard interaction sets in, the magnon dispersion is suppressed and the spectral weight is transferred to the lower boundary of the continuum. With a weak Hubbard interaction as in Fig. 2(b), a bright mode comes out around M, but the spectrum at K still remains as a dim continuum. With the further increase of the Hubbard interaction as in Fig. 2(c), the transferred spectral weight at K eventually concentrates on a roton-like mode with a local minimum in the dispersion. In Figs. 2(d)–2(f), the longitudinal spectra are also presented. From a spectral perspective, one would ascribe the bright mode, emerging adjoint to the bottom of the spinon continuum around Γ′ with gradually weakened spectral peaks approaching the BZ boundary, as the well-defined collective longitudinal modes known as the Higgs modes. Different from the transverse spectra, the longitudinal ones are nearly independent of the Hubbard interaction strength, except that a bright mode would appear around M when a is extremely large [Fig. 2(f)].

To better understand the nature of the modes close to the continuum, we highlight the evolutions of the spectral functions with respect to a for the transverse spin excitations at M/K in Figs. 3(a) and 3(c), and for the longitudinal spin excitations at Γ'/M in Figs. 4(a) and 4(c). Basically, the determination of the magnons and spinons from the spectral perspective is based on the line shape of the spectral function. That is, the sharp Lorentzian quasiparticle peaks are identified as magnons, while the continua with a non-Lorentzian shape adhered to the Lorentzian peak are spinons. Thus, it is empirical. Here we perform the $\alpha = 2$ Rényi entropy calculations with different system sizes and show the results for the quasiparticles with the lowest energies in Figs. 3(b) and 3(d) for the transverse modes at K/M, and in Figs. 4(b) and 4(d) for the longitudinal modes at Γ'/M. There, N is the number of the unit cells along either of the two translation vectors of the honeycomb lattice. Our EE analysis reveals the insufficiency

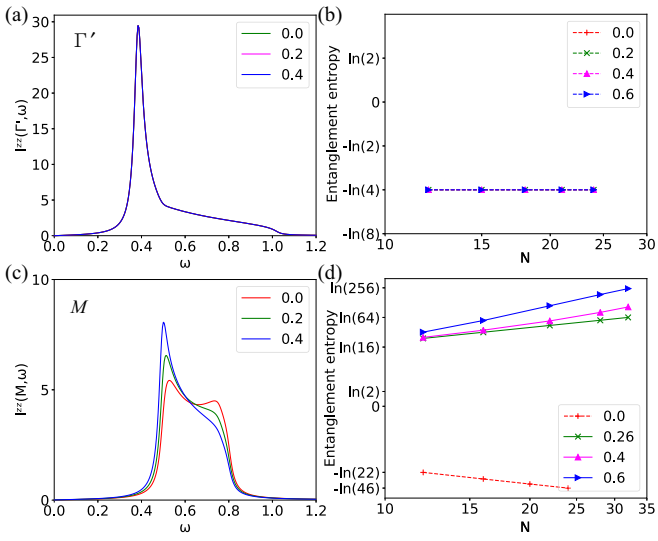

FIG. 4. On the left: longitudinal spectral functions at (a) Γ′ and (c) M. On the right: scalings of the EEs of the lowest longitudinal modes at (b) Γ′ and (d) M.

of the spectral perspective and provides an quantitatively accurate judgment on the confinement and deconfinement of spinons, as will be elaborated below.

For the transverse modes at K [Fig. 3(a)], as has been discussed above, the spectral weight transfers to the lower energy as the Hubbard interaction grows. Besides, the position of the spectral peak changes from the high-energy side to the low-energy side as a grows across $\simeq 0.3$, which corresponds to the emergence of a bright mode in the spectra and is a sign of the avoided fractionalization of the magnons into spinons in the strong interacting regime. This observation is verified by the EE results in Fig. 3(b). As is clearly seen, their EEs converge to constants when $a \lesssim 0.3$ and diverge logarithmically when $a \gtrsim 0.3$. Thus, there is a deconfinement-to-confinement (spinon-to-magnon) transition of the spin excitations across $\simeq 0.3$. In this case, the spectral analysis coincides with the EE analysis. However, for the transverse modes at M, as can be seen in Fig. 3(c), no qualitative change of the line shapes of the spectral functions could be observed when the Hubbard interaction increases, especially from $a = 0$ to $a \simeq 0.03$. It is hard to determine whether magnons are fractionalized into spinons at this point from the spectral perspective. To resolve this dilemma, we have to resort to the EE analysis. As shown in Fig. 3(d), the EE of the lowest-energy mode at M is logarithmically divergent with the system size when the Hubbard interaction exceeds a critical value ($a \simeq 0.03$). Such a specific scaling behavior implies the formation of stable magnons with $a \gtrsim 0.03$. On the other hand, when $a \lesssim 0.03$, the EE scales proportional to $-\ln(N-1)$ up to $N = 30$ [44]. This is related to the $N-1$-fold degeneracy of the lowest-energy spinon particle-hole pairs. For a single mode in the degenerate manifold, the averaged EE converges to a constant. Thus, the spin excitations at M with $a \simeq 0$ are deconfined spinons.

For the longitudinal modes at Γ′, regardless of the Hubbard interaction strength, the spin excitations seem to be well-defined Higgs modes at first sight. After all, they exhibit quite sharp peaks in the spectral function [see Fig. 4(a)]. However, the convergence of the EEs in Fig. 4(b) rebuts this physical picture implied by the spectral function, and $S(\mathbf{q}) = -\ln 4$ denotes four degenerate free spinon particle-hole pair excitations. At M, the case for the longitudinal mode is similar to that of the transverse mode, where the confinement and deconfinement of spinons cannot be determined by the spectral functions due to their continuous evolution with a [see Fig. 4(c)]. By the evaluation of the EEs as in Fig. 4(d), it can be concluded that a stable Higgs mode emerges as $a \gtrsim 0.26$.

In summary, we propose an entanglement entropy analysis to identify the confinement and deconfinement of spin excitations. Applying it to the honeycomb-lattice antiferromagnet, we elaborate quantitatively the deconfinement-to-confinement transition of spinons in the anomalous spectra, indicating the avoided fractionalization of magnons in the strong Hubbard interaction regime. We find the Higgs mode at the Γ′ point is always deconfined as spinons, although it appears as a sharp well-defined quasiparticle from the spectral perspective.

The anomalous continuum of the spin excitations in the recent experiments of $YbCl_3$ and $YbBr_3$ [14–17] is close to the $a = 0.2$–0.3 case in this paper, where the spectra peak at K is more broadening than that at M, and is not pushed down to be a well-defined rotonlike mode. But the experiments do not show a definite bottom of the continuum at K. Thus, the effective models of the two compounds remain to be verified. Moreover, the fluctuations induced by the frustrations may not be limited to the SU(2) RVB type. Investigations beyond the mean-field level is needed to determine whether a Z_2 spin-liquid type is more favorable.

It is noted that there exists another scenario to account for the anomalous spectra in the high-energy region, which is attributed to the magnon damping [17,45–51] instead of the deconfinement of spinons. In principle, the EEs for damped magnons and deconfined spinons should have different scaling behaviors. The EE analysis could be generalized to more unbiased methods in future works to help settle down this debate.

This work was supported by the National Natural Science Foundation of China (Grants No. 11904170, No. 11774152, and No. 12004191), the Natural Science Foundation of Jiangsu Province, China (Grants No. BK20190436 and No. BK20200738), National Key Projects for Research and Development of China (Grant No. 2016YFA0300401), and Doctoral Program of Innovation and Entrepreneurship in Jiangsu Province.

[1] L. Balents, Nature (London) **464**, 199 (2010).
[2] J. D. Reger and A. P. Young, Phys. Rev. B **37**, 5978 (1988).
[3] C. J. Hamer, W. Zheng, and P. Arndt, Phys. Rev. B **46**, 6276 (1992).

[4] P. W. Anderson, G. Baskaran, Z. Zou, and T. Hsu, Phys. Rev. Lett. **58**, 2790 (1987).

[5] N. B. Christensen, H. M. Ronnow, D. F. McMorrow, A. Harrison, T. G. Perring, M. Enderle, R. Coldea, L. P. Regnault, and G. Aeppli, Proc. Natl. Acad. Sci. **104**, 15264 (2007).

[6] B. Dalla Piazza, M. Mourigal, N. B. Christensen, G. J. Nilsen, P. Tregenna-Piggott, T. G. Perring, M. Enderle, D. F. McMorrow, D. A. Ivanov, and H. M. Rønnow, Nat. Phys. **11**, 62 (2015).

[7] N. S. Headings, S. M. Hayden, R. Coldea, and T. G. Perring, Phys. Rev. Lett. **105**, 247001 (2010).

[8] H. D. Zhou, C. Xu, A. M. Hallas, H. J. Silverstein, C. R. Wiebe, I. Umegaki, J. Q. Yan, T. P. Murphy, J.-H. Park, Y. Qiu, J. R. D. Copley, J. S. Gardner, and Y. Takano, Phys. Rev. Lett. **109**, 267206 (2012).

[9] T. Susuki, N. Kurita, T. Tanaka, H. Nojiri, A. Matsuo, K. Kindo, and H. Tanaka, Phys. Rev. Lett. **110**, 267201 (2013).

[10] J. Ma, Y. Kamiya, T. Hong, H. B. Cao, G. Ehlers, W. Tian, C. D. Batista, Z. L. Dun, H. D. Zhou, and M. Matsuda, Phys. Rev. Lett. **116**, 087201 (2016).

[11] S. Ito, N. Kurita, H. Tanaka, S. Ohira-Kawamura, K. Nakajima, S. Itoh, K. Kuwahara, and K. Kakurai, Nat. Commun. **8**, 235 (2017).

[12] Y. Kamiya, L. Ge, T. Hong, Y. Qiu, D. L. Quintero-Castro, Z. Lu, H. B. Cao, M. Matsuda, E. S. Choi, C. D. Batista, M. Mourigal, H. D. Zhou, and J. Ma, Nat. Commun. **9**, 2666 (2018).

[13] Y. Shirata, H. Tanaka, A. Matsuo, and K. Kindo, Phys. Rev. Lett. **108**, 057205 (2012).

[14] J. Xing, E. Feng, Y. Liu, E. Emmanouilidou, C. Hu, J. Liu, D. Graf, A. P. Ramirez, G. Chen, H. Cao, and N. Ni, Phys. Rev. B **102**, 014427 (2020).

[15] C. Wessler, B. Roessli, K. W. Krämer, B. Delley, O. Waldmann, L. Keller, D. Cheptiakov, H. B. Braun, and M. Kenzelmann, npj Quantum Mater. **5**, 85 (2020).

[16] G. Sala, M. B. Stone, B. K. Rai, A. F. May, D. S. Parker, G. B. Halász, Y. Q. Cheng, G. Ehlers, V. O. Garlea, Q. Zhang, M. D. Lumsden, and A. D. Christianson, Phys. Rev. B **100**, 180406(R) (2019).

[17] G. Sala, M. B. Stone, B. K. Rai, A. F. May, P. Laurell, V. O. Garlea, N. P. Butch, M. D. Lumsden, G. Ehlers, G. Pokharel, A. Podlesnyak, D. Mandrus, D. S. Parker, S. Okamoto, G. B. Halász, and A. D. Christianson, Nat. Commun. **12**, 171 (2021).

[18] X.-G. Wen, Phys. Rev. B **65**, 165113 (2002).

[19] W. Zheng, J. O. Fjærestad, R. R. P. Singh, R. H. McKenzie, and R. Coldea, Phys. Rev. Lett. **96**, 057201 (2006).

[20] A. Thomson and S. Sachdev, Phys. Rev. X **8**, 011012 (2018).

[21] F. Ferrari and F. Becca, Phys. Rev. X **9**, 031026 (2019).

[22] C. Zhang and T. Li, Phys. Rev. B **102**, 075108 (2020).

[23] S.-L. Yu, W. Wang, Z.-Y. Dong, Z.-J. Yao, and J.-X. Li, Phys. Rev. B **98**, 134410 (2018).

[24] F. Ferrari and F. Becca, Phys. Rev. B **98**, 100405(R) (2018).

[25] F. Ferrari and F. Becca, J. Phys.: Condens. Matter **32**, 274003 (2020).

[26] T. C. Hsu, Phys. Rev. B **41**, 11379 (1990).

[27] O. F. Syljuåsen and H. M. Rønnow, J. Phys.: Condens. Matter **12**, L405 (2000).

[28] C. M. Ho, V. N. Muthukumar, M. Ogata, and P. W. Anderson, Phys. Rev. Lett. **86**, 1626 (2001).

[29] Y. Tang and A. W. Sandvik, Phys. Rev. Lett. **110**, 217213 (2013).

[30] E. A. Ghioldi, M. G. Gonzalez, L. O. Manuel, and A. E. Trumper, Europhys. Lett. **113**, 57001 (2016).

[31] H. Shao, Y. Q. Qin, S. Capponi, S. Chesi, Z. Y. Meng, and A. W. Sandvik, Phys. Rev. X **7**, 041072 (2017).

[32] M. Gohlke, R. Verresen, R. Moessner, and F. Pollmann, Phys. Rev. Lett. **119**, 157203 (2017).

[33] Z. Y. Meng, T. C. Lang, S. Wessel, F. F. Assaad, and A. Muramatsu, Nature (London) **464**, 847 (2010).

[34] F. Wang, Phys. Rev. B **82**, 024419 (2010).

[35] Y.-M. Lu and Y. Ran, Phys. Rev. B **84**, 024420 (2011).

[36] See Supplemental Material at http://link.aps.org/supplemental/10.1103/PhysRevB.104.L180406 for the mean-field theory of J_1-J_2 Heisenberg model, and the effective Hamiltonian from RPA.

[37] L. Capriotti and S. Sorella, Phys. Rev. Lett. **84**, 3173 (2000).

[38] H. Mosadeq, F. Shahbazi, and S. A. Jafari, J. Phys.: Condens. Matter **23**, 226006 (2011).

[39] R. F. Bishop, P. H. Y. Li, D. J. J. Farnell, and C. E. Campbell, J. Phys.: Condens. Matter **24**, 236002 (2012).

[40] A. Di Ciolo, J. Carrasquilla, F. Becca, M. Rigol, and V. Galitski, Phys. Rev. B **89**, 094413 (2014).

[41] Z. Zhu, D. A. Huse, and S. R. White, Phys. Rev. Lett. **110**, 127205 (2013).

[42] A. Mulder, R. Ganesh, L. Capriotti, and A. Paramekanti, Phys. Rev. B **81**, 214419 (2010).

[43] Z.-Y. Dong, W. Wang, Z.-L. Gu, S.-L. Yu, and J.-X. Li, Phys. Rev. B **102**, 224417 (2020).

[44] Here an extra sum over the degenerate states is applied in Eq. (4) since in numerics the EE for a single mode in the degenerate manifold is not stable due to the degeneracy. Thus, the summed EEs $S \propto -\ln D$ if the excitations are free spinons, where D is the degeneracy.

[45] Y. Li, D. Adroja, R. I. Bewley, D. Voneshen, A. A. Tsirlin, P. Gegenwart, and Q. Zhang, Phys. Rev. Lett. **118**, 107202 (2017).

[46] Z. Zhu, P. A. Maksimov, S. R. White, and A. L. Chernyshev, Phys. Rev. Lett. **119**, 157201 (2017).

[47] Z. Ma, J. Wang, Z.-Y. Dong, J. Zhang, S. Li, S.-H. Zheng, Y. Yu, W. Wang, L. Che, K. Ran, S. Bao, Z. Cai, P. Čermák, A. Schneidewind, S. Yano, J. S. Gardner, X. Lu, S.-L. Yu, J.-M. Liu, S. Li, J.-X. Li, and J. Wen, Phys. Rev. Lett. **120**, 087201 (2018).

[48] A. W. Sandvik and R. R. P. Singh, Phys. Rev. Lett. **86**, 528 (2001).

[49] A. L. Chernyshev and M. E. Zhitomirsky, Phys. Rev. B **79**, 144416 (2009).

[50] M. Mourigal, W. T. Fuhrman, A. L. Chernyshev, and M. E. Zhitomirsky, Phys. Rev. B **88**, 094407 (2013).

[51] M. Powalski, K. P. Schmidt, and G. S. Uhrig, SciPost Phys. **4**, 001 (2018).